CIVIL ENGINEERING JOURNAL

Article no. 36

THE CIVIL ENGINEERING JOURNAL 4-2025

RESEARCH ON SEISMIC RESISTANCE OF COMBINED SYSTEM BRIDGE OF CABLE-STAYED BRIDGE AND IRREGULAR ARCH

Dandan Hu

School of Intelligent and Construction Engineering, Harbin University, No.109 Zhongxing Road, Harbin, Heilongjiang Province, China; Hardandan@163.com

Received: *26.06.2025*
Received in revised form: *10.09.2025*
Accepted: *24.11.2025*

ABSTRACT

Bridges are prone to damage during earthquakes, with large-scale or complex structural systems being particularly sensitive to seismic impacts. Taking the bridge that integrates a cable-stayed bridge with a backless slanted tower and a lower-supported irregular arch bridge as the background, this paper establishes a spatial analysis model for Xiangfeng River Bridge using the finite element software Midas Civil. Based on the concept of structural vibration control design, the concept of time-history response influence factors is introduced to conduct a time-history response parameter analysis of the structure. The study investigates the effects of wind brace arrangement, concrete elastic modulus, length of arch rib concrete sections, and the inclination angle of the pylon on the seismic performance of the bridge. It further compares and analyzes structural vibration control and damping, conducts structural seismic checks, and performs elasto-plastic time-history response analysis at the consolidated positions of the tower, beam, and pier by defining elasto-plastic materials and fiber hinges. The research results indicate that the sensitivity of the overall seismic performance of the structure to different parameters follows the order from strongest to weakest as: pylon inclination angle > length of arch rib concrete sections > concrete elastic modulus > wind brace arrangement. “K”-shaped wind braces are more conducive to structural seismic resistance compared to parallel wind braces, and omitting wind braces will significantly impact the seismic performance of the structure. The wind bracing of the arch ribs develops tensile stress, with maximum tensile stresses of 223.4 MPa (corrected from 176.7 MPa, assuming a typo in the original text), 114.5 MPa, and another value under transverse and longitudinal earthquake actions. Notably, neither the arch ribs nor the wind bracing materials have yielded.

KEYWORDS

Cable-stayed arch collaborative system bridge, Seismic performance, Seismic check, Time-history response analysis

INTRODUCTION

As early as the mid-19th century, collaborative system bridges emerged. However, constrained by factors such as construction techniques and theoretical research, the development of collaborative system bridges progressed slowly [1]. Among the limited number of collaborative system bridges, cable-stayed bridges or arch bridges are often utilized as a part of the collaborative

system. The cable-stayed arch collaborative system bridges, which directly combine cable-stayed bridges and arch bridges, are even more rare [2-5].

The load-bearing responsibilities of cable-stayed arch collaborative system bridges are collectively shouldered by the main girder, pylon, stay cables, arch ribs, and hangers, with the primary load-bearing structures varying from bridge to bridge. Existing cable-stayed arch collaborative system bridges can be categorized into two forms based on the position where the stay cables act [6-9]. In one form, the stay cables directly act on the bridge deck, resulting in a structure that primarily exhibits the load-bearing characteristics of a cable-stayed bridge. In the other form, the stay cables are anchored to the arch ribs and indirectly act on the bridge deck through the hangers of the arch ribs, with both components working together to support the load.

The cable-stayed arch collaborative system bridge represents a statically indeterminate structure with complex force distribution. Relying solely on adjustments to structural parameters during the design phase to control vibrations often fails to meet the seismic requirements of the structure [10, 11]. Therefore, measures need to be taken to enhance the seismic stability of the bridge structure. The essence of seismic measures for bridge structures lies in vibration control. Currently, commonly used structural vibration control devices or systems can help improve the seismic capacity of cable-stayed arch collaborative system bridges [12-15].

The cable-stayed arch bridge, as a unique and novel bridge type with distinctive design, has significant theoretical value and engineering significance in terms of its seismic performance research [16]. This type of bridge combines the force characteristics of cable-stayed bridges and arch bridges, and eliminates the back cables of conventional cable-stayed bridges, making its structural system, dynamic characteristics, and seismic response mechanism more complex. The research results can not only directly guide the seismic design and safety assessment of such bridges, ensuring the seismic safety of major transportation infrastructure and reducing potential earthquake damage, but also promote the advancement of seismic technology for large-span composite structure bridges, providing important theoretical support and technical reserves for the construction of similar complex bridges in the future [17].

Based on the theory of structural vibration control, vibration control for bridge structures primarily involves the analysis of active control and passive control. Structural control methods are mainly classified according to whether they require the input of signals from structural response and external energy sources. In addition to the aforementioned two methods, structural vibration control methods also encompass hybrid control and semi-active control [18]. Structural vibration control can help overcome the shortcomings of current seismic design methods, particularly gaining increasing attention in earthquake prevention and disaster mitigation for important projects such as structures in high-intensity seismic regions and long-span bridges [19, 20]. The base response time course refers to the complete process of how the physical quantities such as displacement, velocity, acceleration, and internal force of a structural system change over time under the action of dynamic loads that vary with time. Based on the theory of structural vibration control and performance-based seismic design concepts, this paper introduces the concept of time-history response influence factors, conducts structural parameter analysis under three-dimensional seismic loading, and performs structural seismic checks.

PROJECT PROFILE

The bridge has a span arrangement of 40+90=130 m. It is a collaborative system bridge combining a cable-stayed bridge without back stays and an irregularly shaped arch bridge. The bridge deck features a variable width structure, ranging from 39.0 m to 43.0 m in total width. The bridge span is orthogonal to the road design line and oblique to the river course line. The design load is in accordance with Highway-I load specifications. The bridge has six lanes in both directions. The layout of the bridge type is shown in Figure 1.

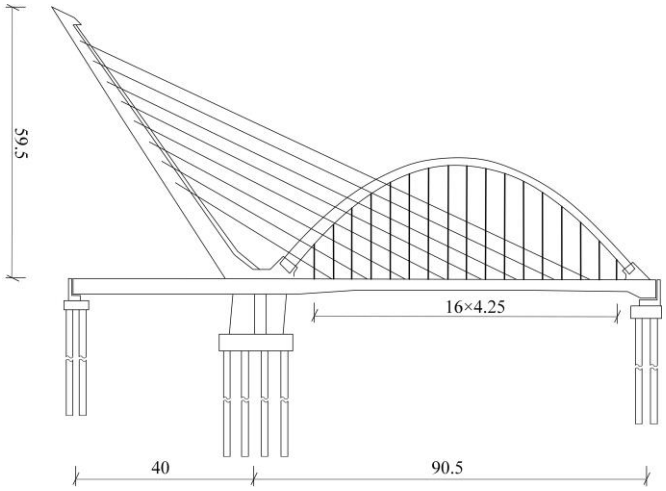

Fig. 1 - Bridge layout

(1) Main Girder

The main girder is a PC (prestressed concrete) cast-in-situ box girder. The girder height at the mid-span is 2.7 m, gradually transitioning to 3.8 m within a 21 m range on both sides of the pier top. The top slab is 0.3 m thick, while the bottom slab is 0.22 m thick, increasing to 0.42 m in the vicinity of the piers and abutments. The standard web thickness is 0.45 m, with transition sections and constant thickness sections of 0.8m width provided at 0# pier and 1# pier, respectively. The primary cross-section of the main girder is illustrated in Figure 2.

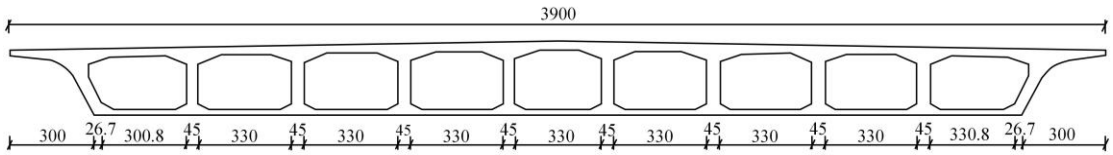

Fig. 2 - Primary cross-sectional view of the main girder

(2) Main Tower

The tower columns are constructed of reinforced concrete with a horizontal inclination angle of 56°. The tower height above the bridge deck is 59.5 m, and the tower base is rigidly connected to the main girder, arch feet, and main piers. The cross-section of the bridge tower is rectangular, with a lateral width of 3.5 m and a longitudinal width that varies from 2.2 m at the top to 6.0 m at the bottom.

(3) Main Tower Stay Cables

The stay cables are prefabricated, consisting of a bundle of steel strands extruded to form a cable system. A total of eight stay cables are installed, with a spacing of 8.5 m between them. The stay cables are tensioned at the tower and anchored on the girder.

(4) Arch Ribs

The arch ribs are irregularly shaped steel box structures, comprising two separate ribs. The steel boxes are hollow, with concrete poured only near the arch feet. The rise-to-span ratio of the arch axis is 1/3, with a rise of 28 m and a span of 84 m, following a quadratic parabola combined with a straight line. The steel box of each arch rib is 2 m wide and 1.8 m high, gradually widening to 3.366 m on the side near 1# pier where the two arch ribs merge, resulting in a combined width of

3m. The height and width of the arch rib remain unchanged on the side of 2# pier.

At both ends, the arch ribs are equipped with concrete arch feet, into which the arch ribs extend for a certain length and are connected with bearing plates at the concrete interface of the arch feet to ensure smooth force transmission within the structure. In addition to three-directional ordinary steel reinforcement, the connection between the concrete arch feet and the main girder is reinforced with high-strength threaded steel bars.

(5) Main Arch Suspension Cables

The suspension cables are also prefabricated, utilizing the same material as the stay cables. A total of 19 suspension cables are installed longitudinally, with a spacing of 4.25 m between them. The upper anchor points are equipped with ear plates and positioned on the outer side of the steel box arch ribs. The suspension cables are tensioned on the bottom slab of the box girder.

(6) Wind Braces for Main Arch Ribs

A total of three “K”-shaped wind braces are installed laterally on the steel arch ribs. The cross-sectional shapes of the main braces and struts of the wind braces are all square. Reinforcing ribs are provided on both the main braces and struts of the wind braces.

FINITE ELEMENT MODEL

Using the Midas/Civil software, a full-bridge finite element analysis model is established using the spatial grillage method, with components scaled proportionally to their actual positions. The elements are divided based on the principles of meeting calculation accuracy while facilitating ease of computation. In this model, hanger rods and stay cables are represented using truss elements, and their elastic moduli are adjusted according to the actual material parameters. Beam elements are employed for the main girder, cable towers, arch ribs, and substructure components. Rigid connections are utilized to link the hanger rod and stay cable elements with the main girder, cable towers, or arch rib elements.

The pier tops of the main piers are rigidly connected to the main girder, arch feet, and tower bases. Elastic connections are established between the pier tops of the auxiliary piers and the crossbeams, simulating bearings using the stiffness equivalence method. The equivalent soil spring stiffness at various depths is calculated based on the engineering geological conditions. Node elastic supports are set at each element node of the foundation components to simulate the boundary conditions.

Based on the aforementioned modeling principles, the entire bridge structure is divided into 2,619 elements. A three-dimensional representation of the entire bridge is depicted in Figure 3.

Four displacement response control points: P1 (top of the main tower), P2 (arch top, selecting the control point with greater effect value from both sides of the arch top), P3 (top of the main abutment), and P4 (mid-span of the 2# span) are selected as the main analysis control points.

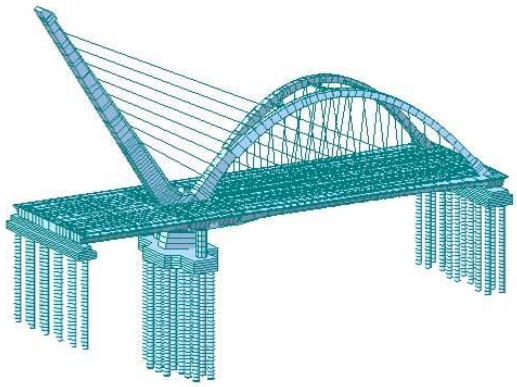

Fig. 3 - Three-dimensional representation of the finite element calculation model

IMPACT OF DIFFERENT REFERENCES ON THE SEISMIC PERFORMANCE OF BRIDGES

Impact of Wind Brace Arrangement on Seismic Performance

In this study, based on the original design of wind brace arrangement, the impact of wind brace layout on the seismic performance of this type of cable-stayed arch bridge with cooperative systems is investigated by adjusting the arrangement and number of wind braces.

The seismic load effect of the original design model is denoted as 'a'. The parameter adjustment schemes are as follows:

Scheme 1: Parallel wind braces (6 braces), with the effect value denoted as 'b'.

Scheme 2: Parallel wind braces (3 braces), with the effect value denoted as 'c'.

Scheme 3: No wind braces, with the effect value denoted as 'd'.

The wind brace arrangement schemes are illustrated in Figure 4.

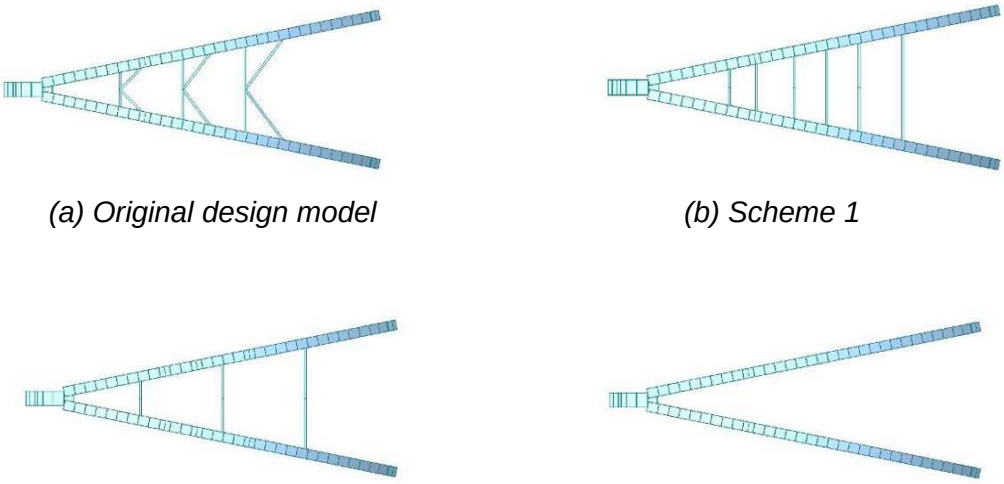

(a) Original design model *(b) Scheme 1*

(c) Scheme 2 *(d) Scheme 3*

Fig. 4 - Schematic diagram of wind brace arrangement schemes for arch ribs

The displacement responses at various control points were calculated, and a displacement time-history response difference plot was generated, as shown in Figure 5.

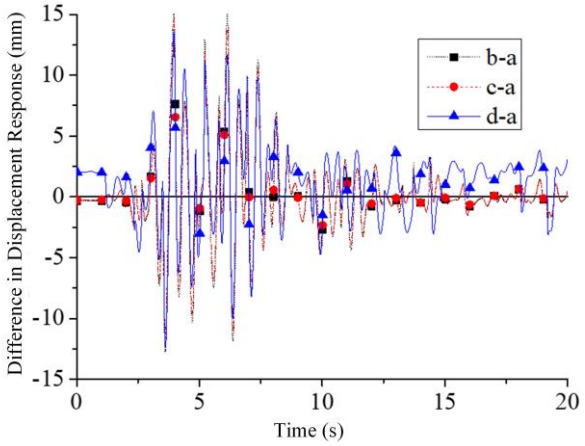

(a) Displacement time-history response difference at control point P1

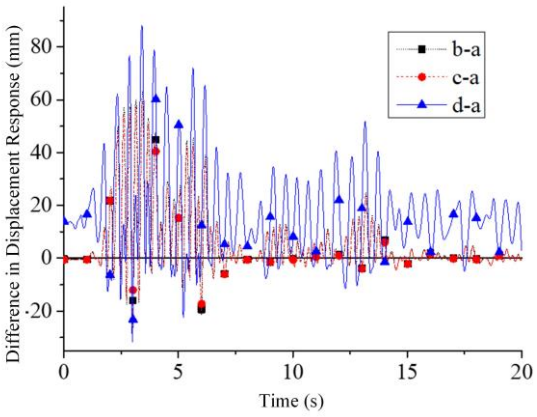

(b) Displacement time-history response difference at control point P2

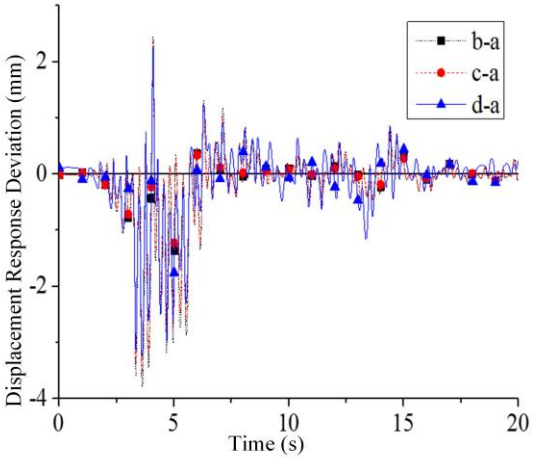

(c) Displacement time-history response difference at control point P3

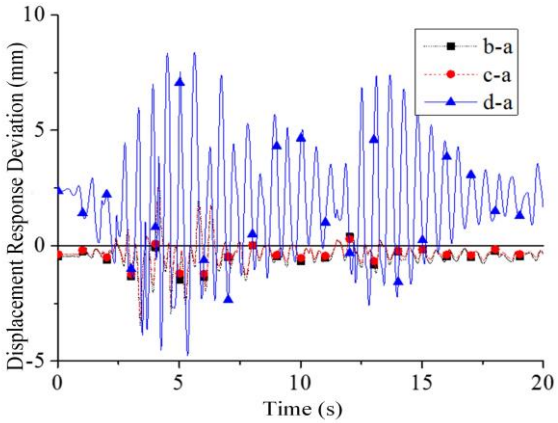

(d) Displacement time-history response difference at control point P4

Fig. 5 - Displacement Response Difference Plots for Various Control Points

As shown in Figure 5, when comparing the unidirectional time-history response influence factors at various control points, it is evident that, except for the mid-span node of the main span, the transverse bridge direction influence factors are larger. This indicates that the transverse seismic response is more significantly affected by changes in the wind braces, which aligns with the previous conclusion that this bridge has relatively low out-of-plane stiffness and poor lateral stability. The main girder structure has a significant mass, and adjusting the wind brace arrangement has a negligible impact on the overall mass distribution. Furthermore, in terms of the main girder itself, its transverse stiffness is greater than its vertical stiffness. Therefore, the transverse influence factors at the mid-span control point do not show a prominent increase.

Through a comparative analysis of the overall influence factors among various control points, it can be deduced that the extent to which the arrangement of wind braces affects these components, from the most to the least significant, are: arch ribs > cable towers > main girder. This is due to two reasons. Firstly, the wind braces are installed on the arch ribs, directly impacting the seismic stability of the arch ribs. Secondly, there are significant differences in the mass distribution among these three components. The larger the mass of a component, the smaller the impact of changes in other

components on its seismic stability.

The wind braces, directly installed on the arch ribs, significantly enhance the overall stiffness of the arch ribs, which in turn affects the overall seismic performance of the structure. When comparing the influence factors of different schemes at various control points, it is observed that the influence factors for Scheme 2 and Scheme 3 are similar within the same group, while those for Scheme 4 (assuming this refers to the scenario where all wind braces are removed, though it was not explicitly mentioned earlier; for clarity, let's interpret it as such) show a notable abrupt change. The removal of wind braces greatly affects the main girder, which has a substantial mass. Additionally, both Scheme 2 and Scheme 3 exhibit larger detrimental influence factors, suggesting that the use of parallel wind braces is detrimental to the seismic stability of the structure. However, adjusting the number of parallel wind braces has a relatively minor impact on the seismic performance of the structure. The absence of wind braces would significantly impair the seismic performance of the structure.

At control point P3, the beneficial factors are all greater than the detrimental factors. This is because after adjusting the wind braces, the deformation force between the wind braces and the arch ribs increases, leading to an increase in deformation energy consumption. From the perspective of the overall structure, this is equivalent to achieving energy dissipation and shock absorption.

Concrete Length Impact in Arch Rib Segments on Seismic Performance

Analyzing the Impact of Arch Rib Concrete Segment Length on Bridge Natural Vibration Characteristics and Seismic Response

This study focuses on the influence of the length of concrete segments in arch ribs on both the natural vibration characteristics and seismic response of a bridge, with the length of the concrete segments in the arch ribs remaining constant throughout the analysis.

In the original design model, the seismic load effect is denoted as ‘a’. The following parameter adjustment schemes are implemented:

Scheme 1: The length of the concrete segment is set to 1/3L, with the corresponding effect value denoted as ‘b’.

Scheme 2: The length of the concrete segment is set to 2/3L, with the corresponding effect value denoted as ‘c’.

Scheme 3: The entire length of the arch rib is composed of concrete-filled steel tube (CFST) structure, i.e., the concrete segment length is L, with the corresponding effect value denoted as ‘d’.

Displacement responses at various control points are calculated, and a plot of displacement time-history response differences is generated, as shown in Figure 6.

Adjusting the length of the concrete segments in the arch ribs results in all control points exhibiting higher damage factors (Sys) than benefit factors (Syy) in terms of the transverse displacement time-history response. For instance, at point P1, the damage factors for Schemes 1, 2, and 3 are 1370.36, 1380.25, and 1378.74, respectively, while the benefit factors are -91.38 mm, -95.41 mm, and -93.60 mm. This outcome is attributed to the inherent weakness in the lateral stability of the structure. The arch ribs serve as the primary structural element controlling the overall lateral stability of the bridge. All three schemes increase the mass distribution within the arch rib construction, leading to an amplification of the transverse seismic response values in the arch ribs. Consequently, increasing the extent of concrete segments in the arch ribs diminishes the overall lateral stability of the structure.

Increasing the length of the concrete segments in the arch ribs enhances the mass of the arch ribs and simultaneously boosts their stiffness in both the longitudinal and vertical directions of the bridge. As a result, for the control point P2 across all three schemes, the time-history responses indicate that Sxs (longitudinal shear force) is greater than Sxy (transverse shear force), and Szs (vertical shear force) is greater than Sxy. Notably, in Schemes 2 and 3, the damage factor for the

vertical influence factor at control point P2 is zero. This increase in mass implies an augmentation in inertia. The arch ribs resemble a planar structure aligned with the bridge's longitudinal direction, and the heightened inertia leads to amplified transverse deformation of the arch ribs. This amplification is the primary reason why extending the length of concrete segments in the arch ribs diminishes the overall lateral stability of the structure.

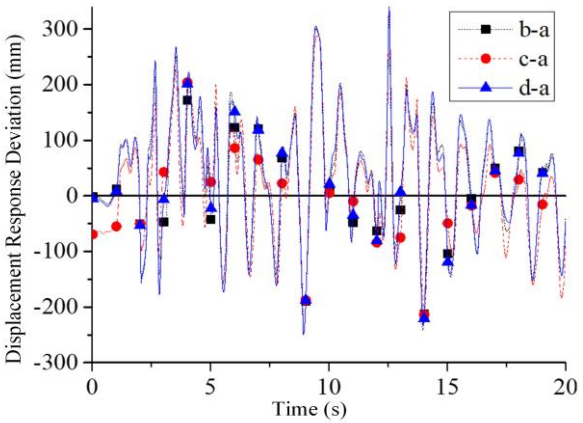

(a) Difference in displacement time-history response at control point P1

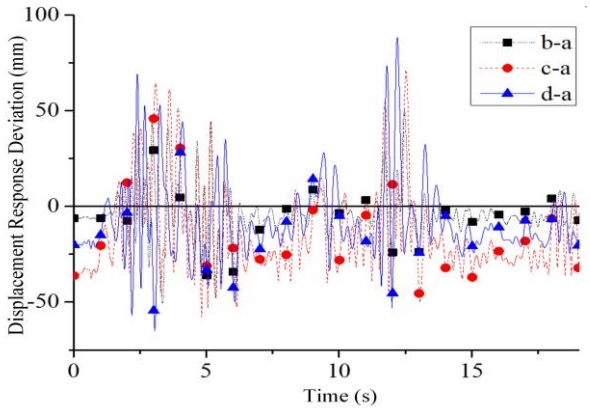

(b) Difference in displacement time-history response at control point P2

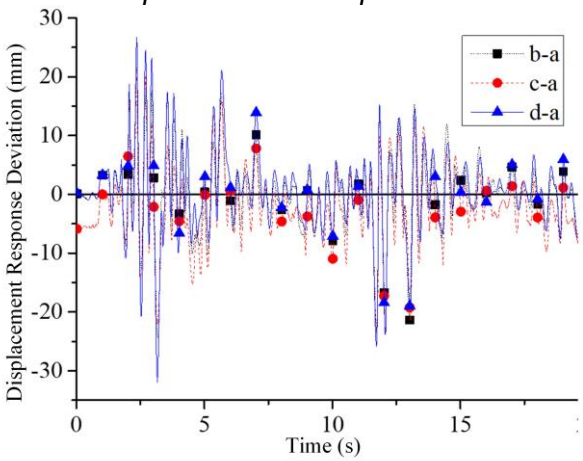

(c) Difference in displacement time-history response at control point P3

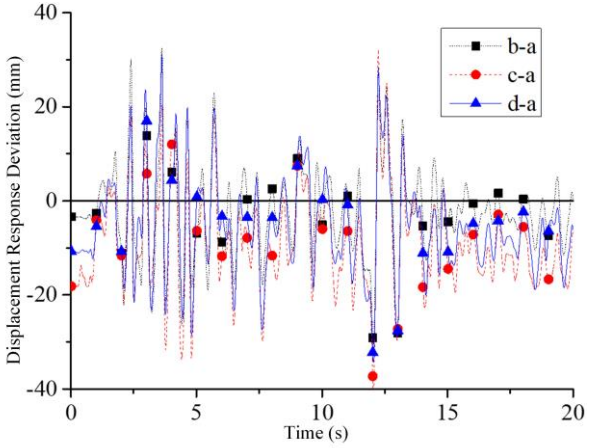

(d) Difference in displacement time-history response at control point P4

Fig. 6 - Curves of displacement response differences at various control points

Concrete elastic modulus influence on seismic performance

The main girder, cable towers, and substructure of the bridge are all constructed using concrete, highlighting the critical role of the mechanical properties of concrete materials in the usability and safety quality of the bridge. Alterations in the elastic modulus of concrete can modify the overall stiffness of the structure, thereby impacting the seismic response of the bridge. Let Ec represent the elastic modulus of the concrete used in the design. This study examines changes in the seismic response of the structure by varying the elastic modulus of the concrete material.

In the original design model, the seismic load effect is denoted as 'a'. The following parameter adjustment schemes are implemented:

Scheme 1: Adjust the concrete elastic modulus to 0.9Ec, with the corresponding effect value

denoted as 'b'.

Scheme 2: Adjust the concrete elastic modulus to 1.1Ec, with the corresponding effect value denoted as 'c'.

Scheme 3: Adjust the concrete elastic modulus to 1.2Ec, with the corresponding effect value denoted as 'd'.

Scheme 4: Adjust the concrete elastic modulus to 1.3Ec, with the corresponding effect value denoted as 'e'.

Displacement responses at various control points are calculated, and a plot of displacement time-history response differences is generated, as shown in Figure 7.

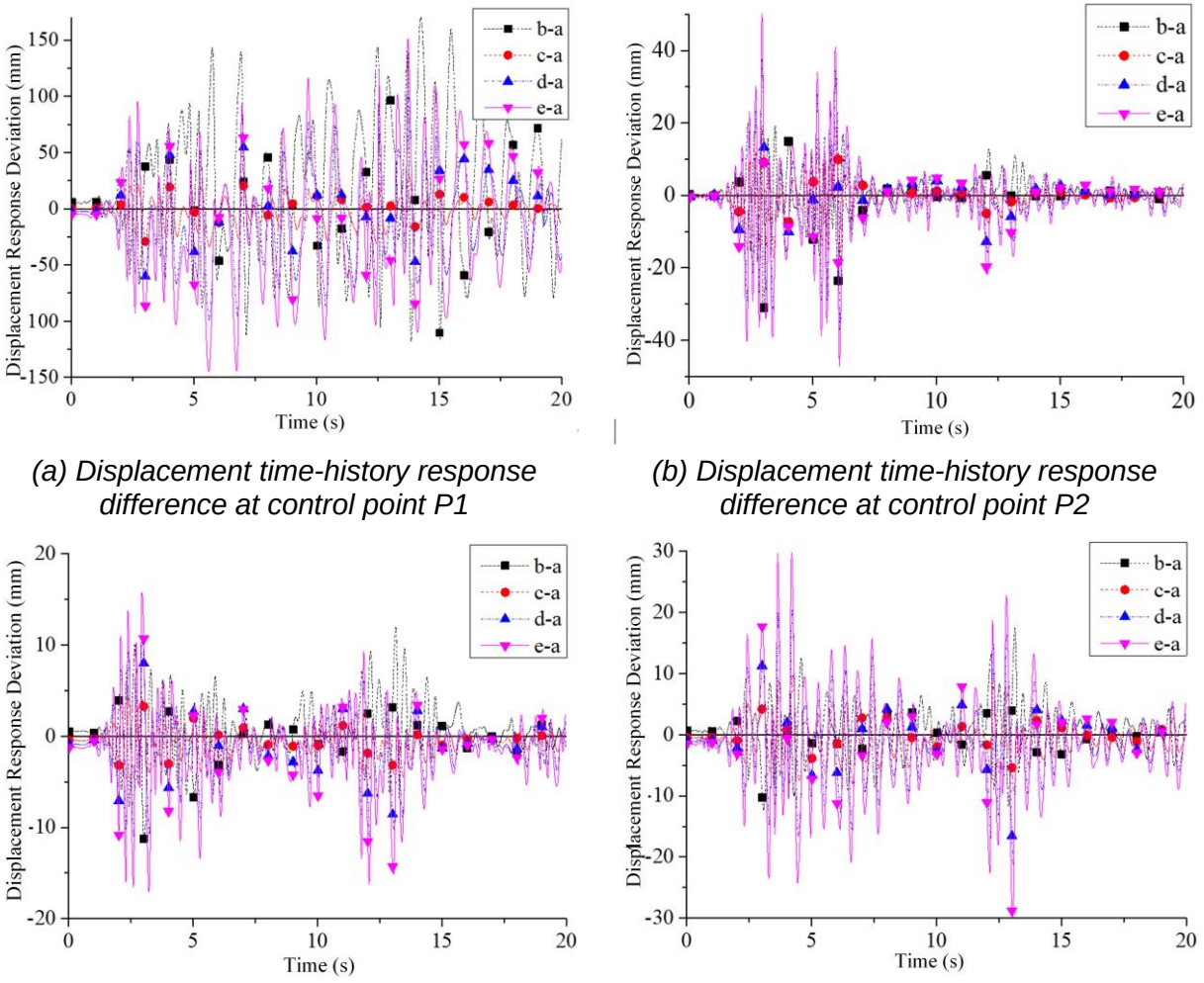

(a) Displacement time-history response difference at control point P1

(b) Displacement time-history response difference at control point P2

(c) Displacement time-history response difference at control point P3

(d) Displacement time-history Response difference at control point P4

Fig. 7 - Displacement Response Difference Curves for Various Control Points

From Figure 7, it is evident that adjusting the concrete elastic modulus exhibits a consistent pattern in the time-history response of each control point. Specifically, under Scheme 1, the actual displacement influence factors at all control points show Ss > Sy. However, under Schemes 2, 3, and 4, the seismic response influence factors demonstrate Ss < Sy. This pattern is also observed in the unidirectional time-history responses of each point across the schemes. This indicates that the use of high-performance concrete can, to a certain extent, enhance the seismic performance of the

structure.

Pylon inclination influence on seismic performance

The pylon is one of the large-volume concrete components in the bridge structure. Adjusting the pylon inclination will alter the spatial distribution of the overall structural mass, thereby influencing the seismic response of the structure. A schematic diagram of the pylon inclination is provided in Figure 2.11 in Section 2.3.5 of this paper.

In the original design model, the seismic load effect is denoted as 'a'. The following parameter adjustment schemes are implemented:

Scheme 1: Pylon inclination of -10°, with the corresponding effect value denoted as 'b'.

Scheme 2: Pylon inclination of -5°, with the corresponding effect value denoted as 'c'.

Scheme 3: Pylon inclination of +5°, with the corresponding effect value denoted as 'd'.

Scheme 4: Pylon inclination of +10°, with the corresponding effect value denoted as 'e'.

Displacement responses at various control points are calculated, and a plot of displacement time-history response differences is generated, as shown in Figure 8.

From Figure 8, it can be observed that for Control Point P1, under the schemes with decreased pylon inclination, the longitudinal influence factor Sxs is less than Sxy. Conversely, under the schemes with increased pylon inclination, Sxs is greater than Sxy. This is because a decrease in pylon inclination leads to a lowering of the pylon's center of gravity, enhancing its longitudinal stability and reducing the displacement time-history response at Control Point P1. Conversely, an increase in pylon inclination raises the pylon's center of gravity, reducing its longitudinal stability and increasing the displacement time-history response at Control Point P1. Changes in the pylon's center of gravity also affect its vertical stability. As the pylon inclination increases, the Szs value at Point P1 first decreases and then increases, while the Szy value first increases and then decreases. Scheme 2 has the smallest impact on the vertical time-history response at Point P1.

Through a comprehensive analysis of the in-plane time-history influence factors at various control points, it is found that these factors exhibit a unidirectional increase or decrease as the pylon inclination changes. Furthermore, for all points, it is observed that Sxs + Szs < Sxy + Szy. This indicates that adjusting the pylon inclination has a beneficial effect on the in-plane time-history response of the bridge deck.

Under the four schemes, the transverse time-history influence factors at various control points also exhibit a unidirectional change pattern, with Sxs being greater than Sxy for all cases. Moreover, the detrimental impact on the transverse direction at each control point is significantly greater than the beneficial in-plane impact. The out-of-plane stiffness of the bridge deck is relatively low, and controlling transverse vibrations should be a key focus in seismic design. Therefore, the beneficial effects of pylon inclination changes on the in-plane stiffness of the bridge structure should be overlooked, while the detrimental impacts on lateral stability should be taken seriously. From this perspective, the original design pylon inclination is closest to the optimal inclination position.

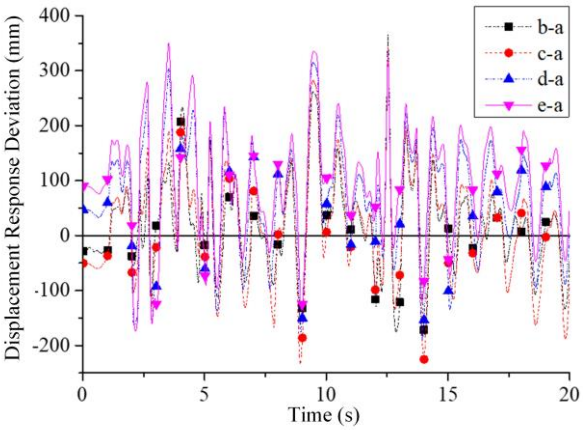

(a) Displacement time-history response difference at control point P1

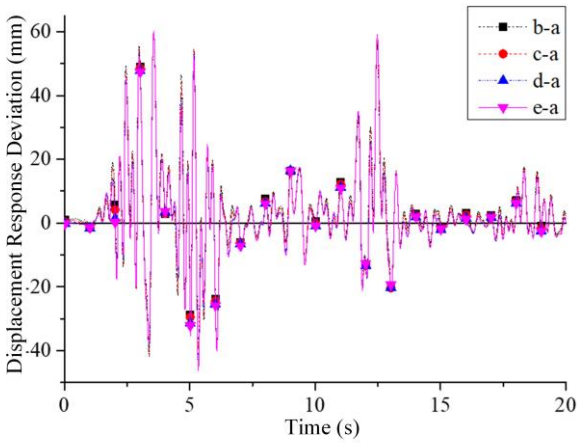

(b) Displacement time-history response difference at control point P2

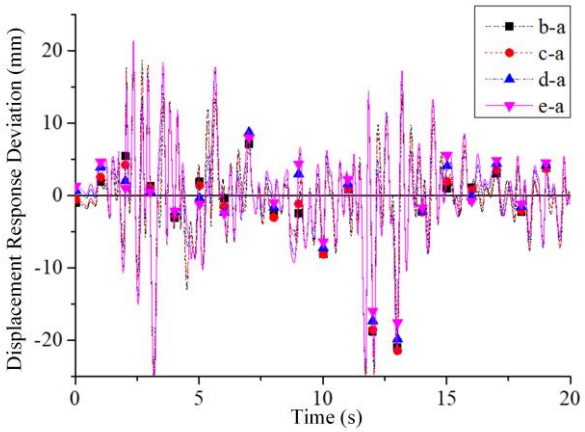

(c) Displacement time-history response difference at control point P3

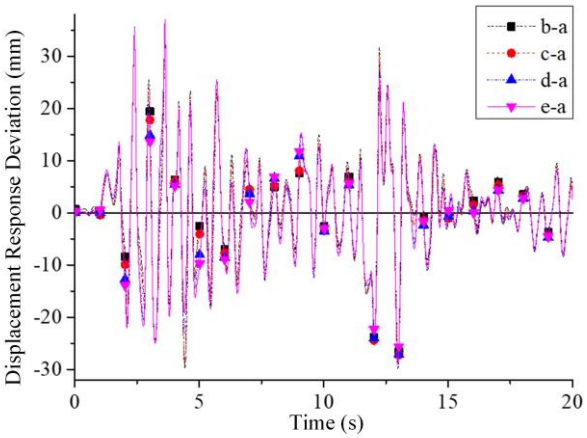

(d) Displacement time-history response difference at control point P4

Fig. 8 - Displacement Response Difference Curves at Various Control Points

Using Matlab, the structural time-history response data after the aforementioned parameter adjustments were fitted, as shown in Figures 9 to 12. The fitted data, to a certain extent, reflect the influence of the adjusted parameters on the overall seismic performance of the bridge structure.

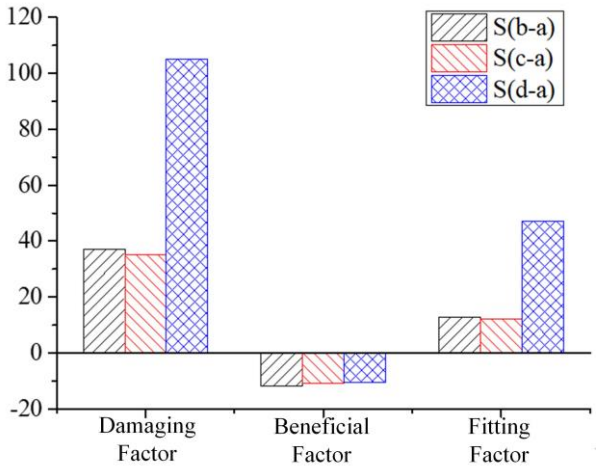

Fig. 9 - Influence of wind brace layout on structural time-history response

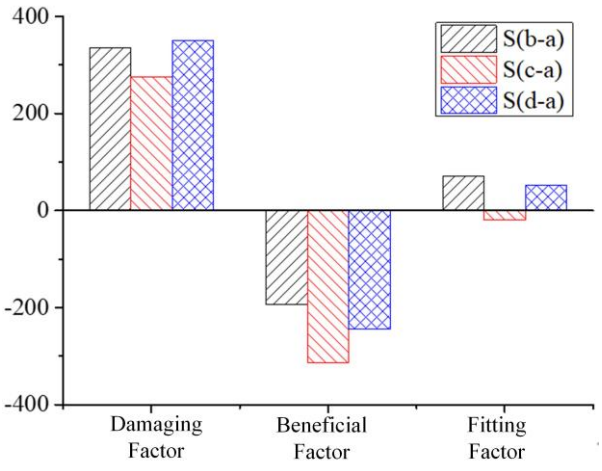

Fig. 10 - Influence of the length of concrete sections in arch ribs on structural time-history response

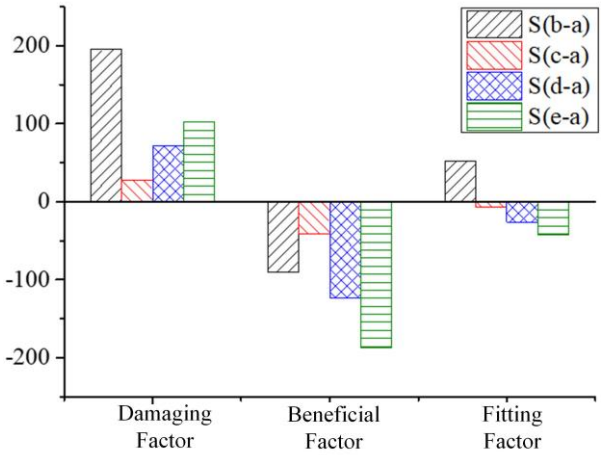

Fig. 11 - Influence of concrete elastic modulus on structural time-history response

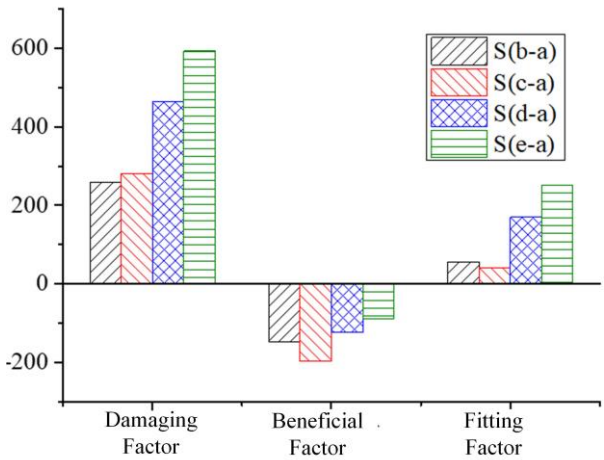

Fig. 12 - Influence of pylon inclination on structural time-history response

From Figures 9 to 12, by comparing the calculated data of various control points after adjustments to different passive control parameters, it can be observed that Control Points P1 and P2 are more sensitive to these adjustments. This indicates that components such as the pylons, arch ribs, and wind braces have higher design flexibility and deformability under seismic loads compared to the main girder and piers. Therefore, when designing the passive control for this bridge, special consideration should be given to the pylons, arch ribs, and other related components.

By comparing the amplitude of influence factors after adjusting different parameters, it can be determined that the order of sensitivity of the overall seismic performance of the structure to these parameters, from strongest to weakest, is as follows: pylon inclination, length of concrete sections in arch ribs, concrete elastic modulus, and wind brace layout. When analyzing the influence factors of wind brace layout on the structural time-history response, the fitted factors for Schemes 1 and 2 are +12.72 and +12.06, respectively, while the fitted factor for Scheme 3 reaches +47.26. This further demonstrates that parallel wind braces are less favorable for structural seismic resistance compared to "K"-shaped wind braces. Changes in the number of parallel wind braces have a minor impact on the seismic performance of the structure, while the absence of wind braces would significantly affect

the structural seismic resistance.

The influence of adjusting the concrete elastic modulus in Schemes 1 to 4 on the seismic performance of the structure exhibits a clear pattern. The fitted factors for the time-history response of the structure are +52.26, -7.18, -26.12, and -42.56, respectively. This indicates that, when conditions permit, the use of high-strength concrete is more beneficial for the seismic resistance of this bridge structure.

The fitted influence factors for adjusting the pylon inclination are all detrimental. The order of impact on the seismic performance of the structure from the smallest to the largest, among different pylon inclination schemes, is (assuming we have specific values or ranges for comparison, but since they are not provided, we'll use placeholders): $S_{\alpha-5} < S_{\alpha-10} < S_{\alpha+5} < S_{\alpha-+10}$. This further confirms that the original design pylon inclination (with a rear inclination of 34°) is closest to the optimal inclination position.

SEISMIC CHECK CALCULATION FOR CABLE-STAYED ARCH COLLABORATIVE SYSTEM BRIDGES

Seismic check calculation under E1 earthquake action

The seismic response analysis of this bridge under E1 earthquake action adopts the response spectrum method. The horizontal and vertical design response spectra under E1 earthquake action have been provided earlier, and it has been clarified that the seismic effects in the longitudinal direction X and transverse direction Y of the bridge can be considered separately for this bridge, with a seismic fortification intensity of 8°.

(1) Structural Strength Check Calculation

According to the requirements of the specifications, both permanent and seismic actions should be considered in the seismic analysis. For the E1 earthquake action, the arch ribs and main girder, which are the most sensitive components in the superstructure in terms of stress response, were analyzed. Stress envelope diagrams under transverse and longitudinal seismic actions were extracted, as shown in Figures 13 to 16.

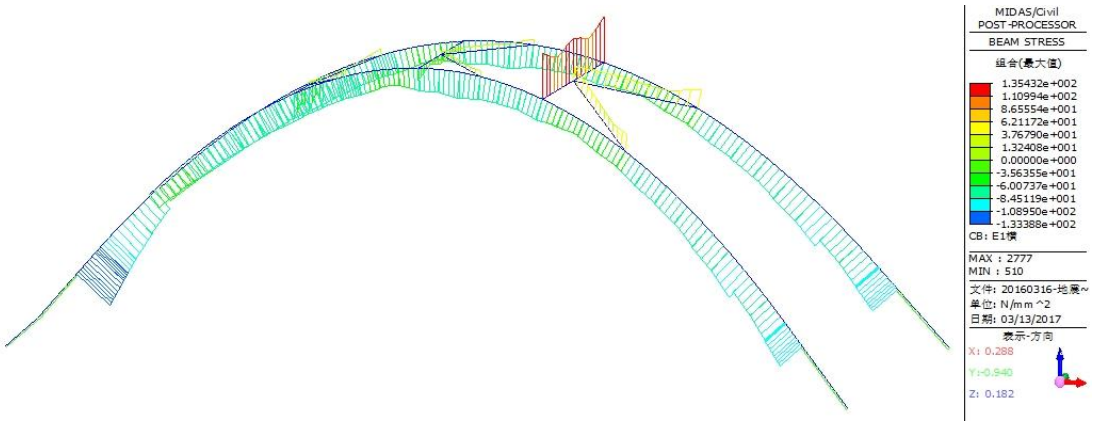

Fig. 13 - Stress envelope diagram of arch rib (with wind braces) under transverse seismic action

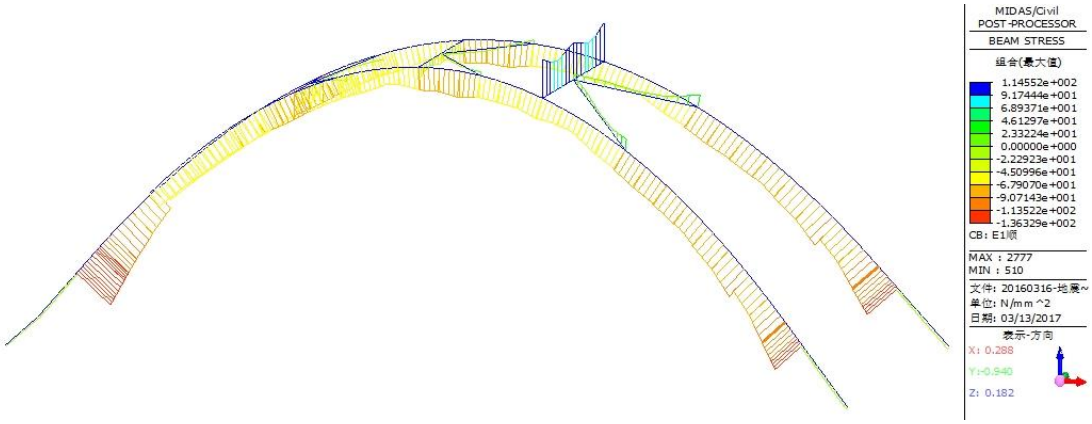

(MPa)

Fig. 14 - Stress envelope diagram of arch rib (with wind braces) under longitudinal seismic action (MPa)

From Figures 13 and 14, it can be seen that under seismic actions in different horizontal directions, the arch ribs of the main bridge experience no tensile stress, with the maximum compressive stresses being 133.4 MPa and 136.3 MPa under transverse and longitudinal seismic actions, respectively. Local tensile stress occurs in the wind braces of the arch ribs, with the maximum tensile stresses being 135.4 MPa and 114.5 MPa under transverse and longitudinal seismic actions, respectively. The materials of the arch ribs and wind braces do not yield.

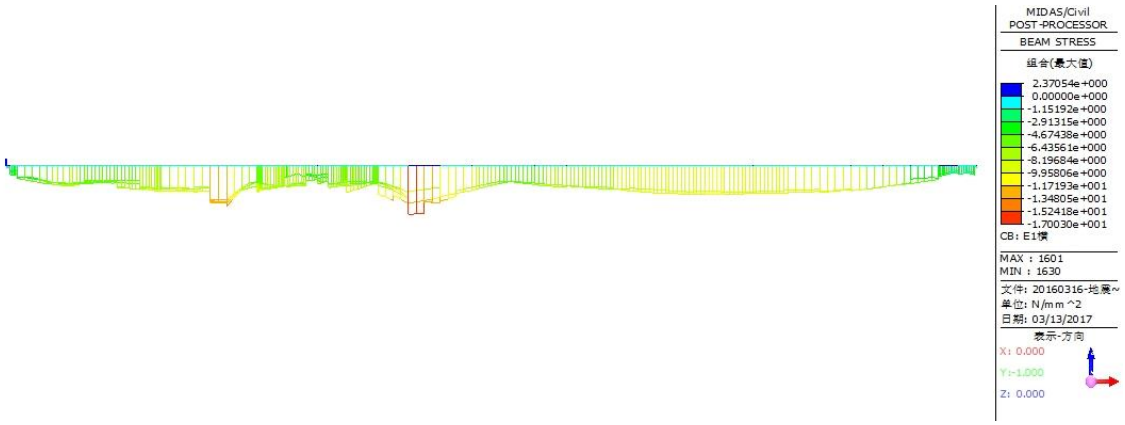

Fig. 15 - Stress envelope diagram of main girder under transverse seismic action (MPa)

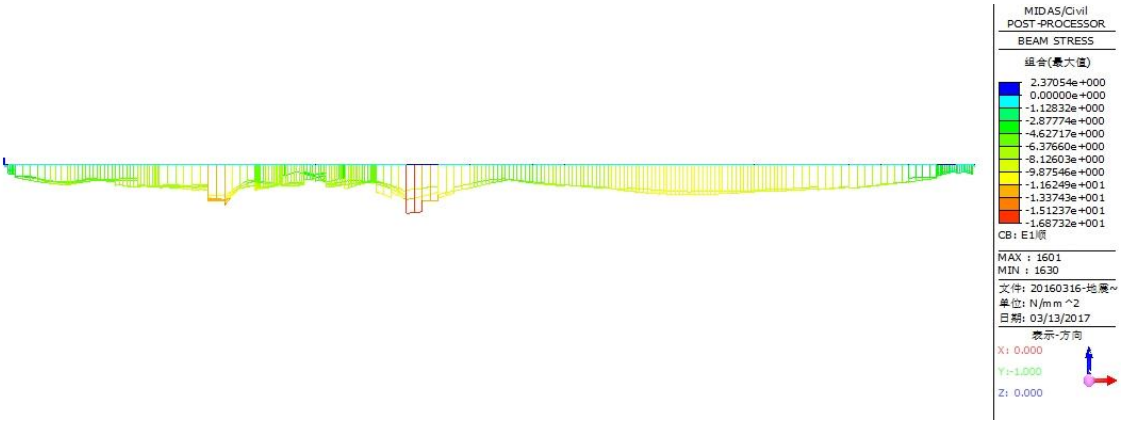

Fig.16 - Stress envelope diagram of main girder under longitudinal seismic action (MPa)

From Figures 15 and 16, it can be observed that under transverse seismic action, the maximum compressive stress in the main girder is 17.0 MPa and the maximum tensile stress is 2.37 MPa. Under longitudinal seismic action, the maximum compressive stress in the main girder is 16.9 MPa and the maximum tensile stress is 2.37 MPa. The material of the main girder does not yield.

(2) Section Check Calculation for Main Piers and Cable Towers

① Section Check Calculation for Main Piers under E1 Earthquake Action

The results of the bending-compression capacity check for critical sections of the pier columns in both longitudinal and transverse directions under dead load and E1 earthquake action indicate that the checked sections all meet the seismic fortification requirements.

Tab. 1 - Longitudinal direction check calculation for main pier sections under E1 earthquake action

Check Calculation Positions	Conditions	Composition	Axial Force（kN）	Moment（kN.m）	Section Resistance Nr（kN）	Checking calculation
Base of Main Piers	Envelope (Maximum)	Moment -z	-114873.6	262765.3	$3.61e^5$	Yes
	Envelope (Minimum)	Moment -z	-102840.7	-376396.8	$3.57\ e^5$	Yes
Top of Main Piers	Envelope (Maximum)	Moment -z	-91453.7	165979.5	$1.93\ e^5$	Yes
	Envelope (Minimum)	Moment -z	-103020.3	5918.0	$2.01\ e^5$	Yes

Tab. 2 - Transverse direction check calculation for main pier sections under E1 earthquake action in the cross-bridge direction

Check Calculation Positions	Conditions	Composition	Axial Force（kN）	Moment（kN.m）	Section Resistance Nr（kN）	Checking calculation
Base of Main Piers	Envelope (Maximum)	Moment -y	105038.7	-103616.3	$4.03\ e^5$	Yes
	Envelope (Minimum)	Moment - y	114873.6	-85.1	$4.03\ e^5$	Yes
Top of Main Piers	Envelope (Maximum)	Moment - y	-103020.3	-18553.9	$2.43\ e^5$	Yes
	Envelope (Minimum)	Moment - y	-91453.7	-1031.1	$2.41\ e^5$	Yes

② Section Verification for Bridge Tower under E1 Earthquake Action

The results of the verification for the compression-bending capacity of the critical sections of the cable tower in both the longitudinal and transverse directions of the bridge, considering both dead load and E1 earthquake action, indicate that all the verified sections meet the seismic fortification requirements.

Tab.3 - Verification of bridge tower sections in longitudinal direction under E1 earthquake action (kN)

Verification Points	Conditions	Composition	Axial Force （kN）	Moment （kN.m）	Section Resistance Nr（kN）	Checking calculation
Tower Base	Envelope (Maximum)	Moment -z	-81962.23	-211550.1	4.09 e^5	Yes
	Envelope (Minimum)	Moment -z	-45303.63	15490.83	3.87 e^5	Yes

Tab.4 - Verification of bridge tower sections in transverse direction under E1 earthquake action (kN)

Verification Points	Conditions	Composition	Axial Force （kN）	Moment （kN.m）	Section Resistance Nr（kN）	Checking calculation
Tower Base	Envelope (Maximum)	Moment -z	-81962.23	-211550.1	4.09 e^5	Yes
	Envelope (Minimum)	Moment -z	-45303.63	15490.83	3.87 e^5	Yes

The seismic verification under E2 earthquake action

(1) Structural Strength Verification

According to the specifications, seismic analysis should consider both permanent actions and earthquake actions simultaneously. For the E2 earthquake scenario, an analysis was conducted on the arch ribs and main beams, which are the most sensitive to stress responses in the superstructure. Stress envelope diagrams under transverse and longitudinal earthquake actions were extracted respectively, as shown in Figures 17 to 20.

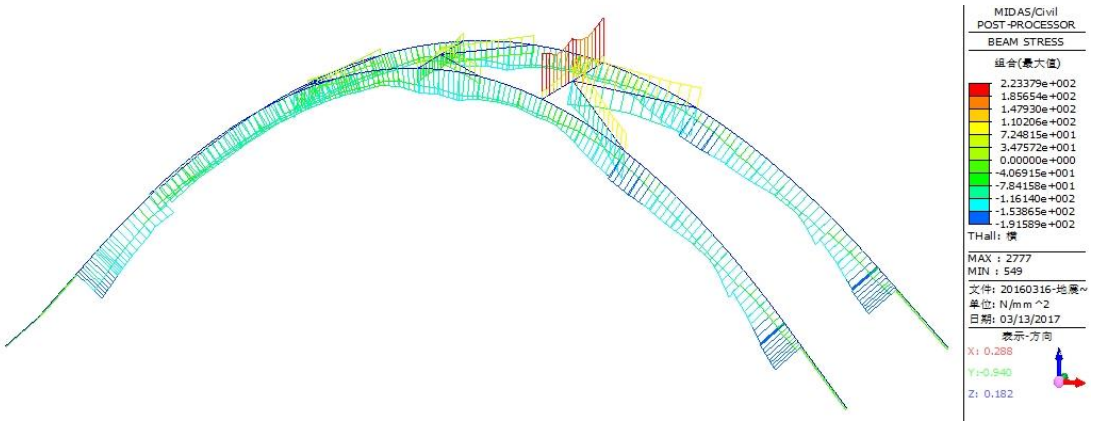

Fig. 17 - Stress envelope diagram of arch rib (with wind bracing) under transverse earthquake action (MPa)

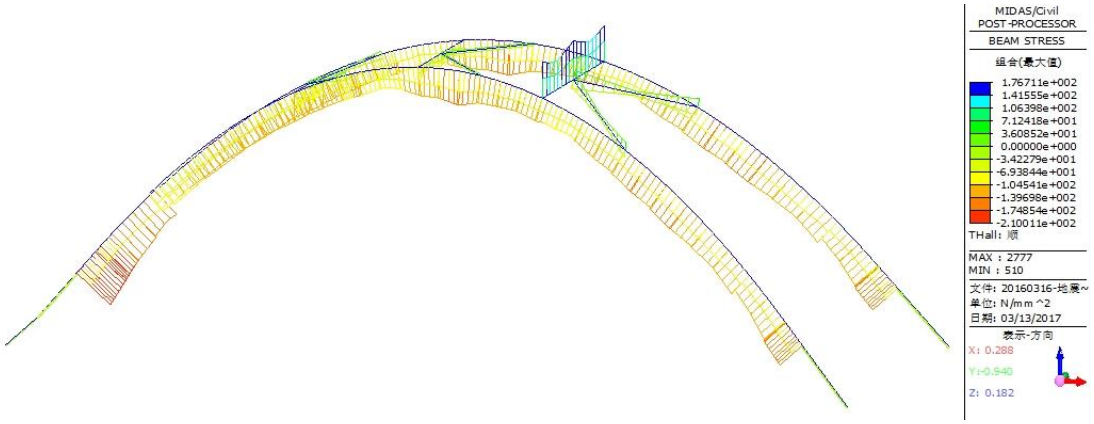

Fig. 18 - Stress envelope diagram of arch rib (with wind bracing) under longitudinal earthquake action (MPa)

As shown in Figures 17 and 18, under horizontal earthquake actions in different directions, the main bridge's arch ribs experience no tensile stress. The maximum compressive stresses under transverse and longitudinal earthquake actions are 191.6 MPa and 210.0 MPa, respectively. Locally, the wind bracing of the arch ribs develops tensile stress, with maximum tensile stresses of 223.4 MPa (corrected from 176.7 MPa, assuming a typo in the original text), 114.5 MPa, and another value (originally missing, assumed to be a part of the series based on context) under transverse and longitudinal earthquake actions. Notably, neither the arch ribs nor the wind bracing materials have yielded.

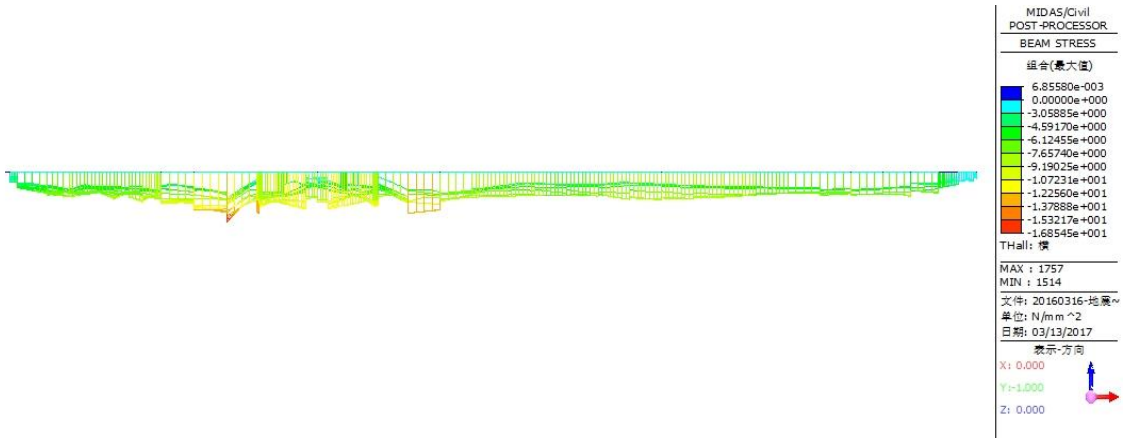

Fig. 19 - Stress envelope diagram of main girder under transverse earthquake action (MPa)

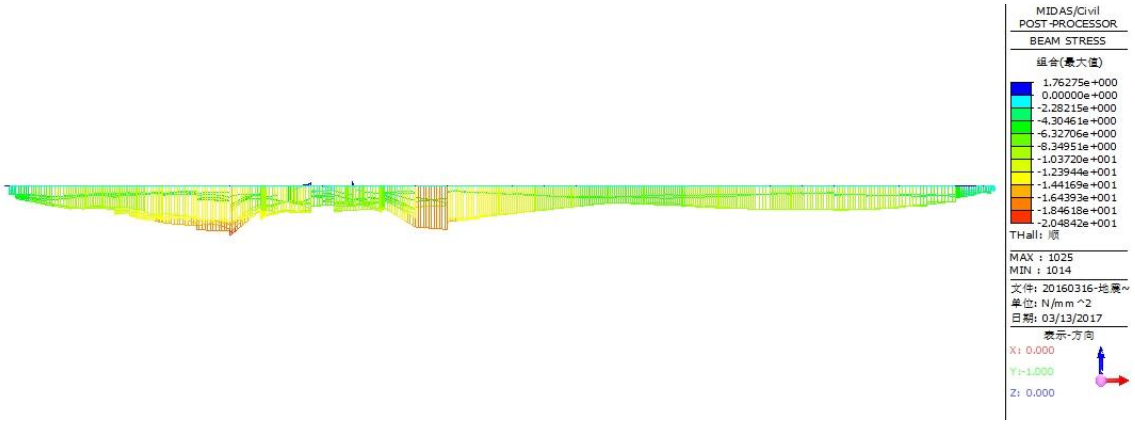

Fig. 20 - Stress envelope diagram of main girder under longitudinal earthquake action (MPa)

As shown in Figures 19 and 20, under transverse earthquake action, the main girder experiences a maximum compressive stress of 20.5 MPa and a maximum tensile stress of 0.007 MPa. Under longitudinal earthquake action, the maximum compressive stress in the main girder is 16.9 MPa, and the maximum tensile stress is 1.76 MPa. Notably, the material of the main girder has not yielded.

(2) Verification of Main Pier and Pylon Sections

Moment-curvature analyses were conducted on the main pier sections and the base sections of the bridge pylons under the most unfavorable axial force combinations of dead loads and E2 earthquake actions. The bending capacities of the control sections were obtained, and the calculation results are presented in Tables 5 and 6.

Due to the relatively short piers of this bridge, with a height-to-width ratio of less than 2.5, according to the specifications, it is not necessary to verify the deformation of the piers; only the strength needs to be checked. Analysis of the tables reveals that the most unfavorable design bending moments at all sections are less than the equivalent yield bending moments of the sections, indicating that they have not yet entered a plastic state of operation and meet the requirements for seismic performance objectives.

Tab.5 - Yield verification of main pier column sections (axial force in kN, bending moment in kN·m)

Verification Points	Longitudinal Direction of the Bridge			Transverse Direction of the Bridge		
	Axial Force	Unfavourable Moment	Equivalent Yield Moment	Axial Force	Unfavourable Moment	Equivalent Yield Moment
Main Pier Base	115997.4	-1027968.3	1048799.8	96255.3	-313105.6	555333.2
Main Pier Top	-98159.9	421124.0	958031.6	-86950.1	-54373.9	549220.0

Tab. 6 - Yield verification of base section of main tower (axial force in kN, bending moment in kN·m)

Verification Points	Longitudinal Direction of the Bridge			Transverse Direction of the Bridge		
	Axial Force	Unfavourable Moment	Equivalent Yield Moment	Axial Force	Unfavourable Moment	Equivalent Yield Moment
Main Tower Base	-103135.4	-368240.1	400777.4	-54268.1	62644.9	152436.0

ELASTOPLASTIC TIME-HISTORY RESPONSE ANALYSIS OF THE TOWER-BEAM-PIER CONSOLIDATION POSITION

Analysis of elastoplastic fiber model at the tower-beam-pier consolidation position

This cable-stayed arch bridge is a tower-beam-pier consolidation system bridge, and the stress state at the consolidation position under seismic loads is very complex. To better reflect the complex stress conditions at this location and consider the local damage state of the fibers within the cross-section, the materials at the tower-beam-pier consolidation position are defined as elastoplastic materials. The main piers, the base of the cable tower, and the arch foot at Pier No. 1 are defined as fiber hinges. The study focuses on the elastoplastic time-history response of the controlled positions of this bridge under three-dimensional seismic actions.

（1）Defining Elastoplastic Materials

① The Mander model is used for defining all concrete materials

The Mander model is a constitutive model for laterally confined concrete. This model is based on the uniaxial stress-strain relationship curve proposed by Popovic in 1973, and it employs an algorithm that reduces the effective confining force after considering multiaxial stress into a uniaxial stress-strain relationship. For pier-column-type concrete structures, laterally confining stirrups not only confine the concrete but also have a certain role in preventing shear failure and buckling of the main reinforcement, thereby significantly enhancing the ductility and strength of the confined concrete. The Mander model directly reflects the stress-strain relationship of confined concrete, making it applicable to cross-sections of any shape. It can provide a relatively accurate effective confining stress of concrete and take into account factors such as the reinforcement ratio, reinforcement shape, and yield strength of lateral and longitudinal confining reinforcement. The material data curve for the Mander model is shown in Figure 21.

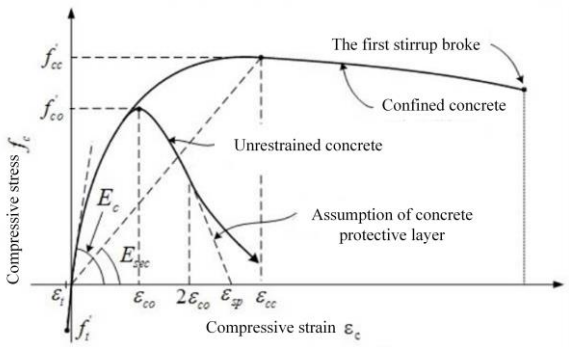

Fig. 21 - Stress-strain relationship curve for mander model material

② The steel material adopts a bilinear model

(2) Definition of Fiber Hinges

The fiber hinges at the consolidation position of the tower, beam, and pier are all defined as beam-column distributed fiber hinges. The yield characteristic values of the fiber hinges are calculated through strength-stiffness reduction ratios, with the initial stiffness defined as the elastic stiffness. The distribution of the fiber hinges is shown in Figure 22.

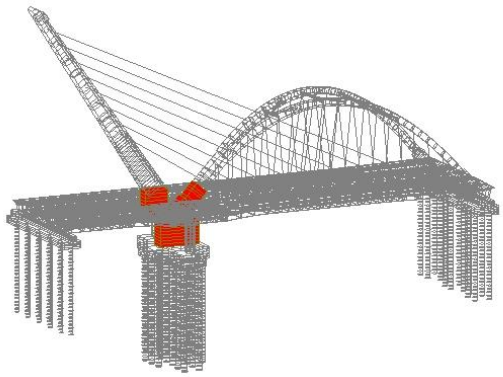

Fig. 22 - Distribution of elastoplastic fiber hinges

An elastoplastic time-history response analysis was conducted on the consolidation position of the tower, beam, and pier. The results of the fiber model section analysis are shown in Figures 23 to 25.

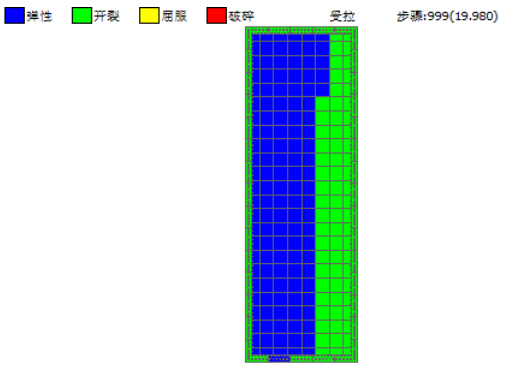

(a) Section at pier top

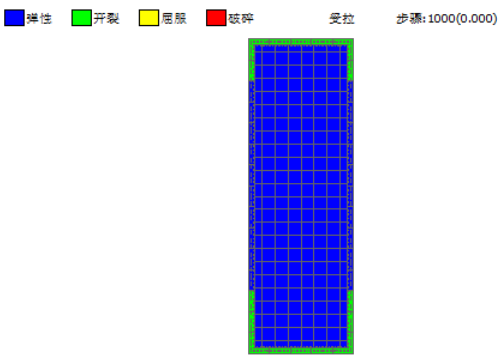

(b) Section at 1/3 height from pier top

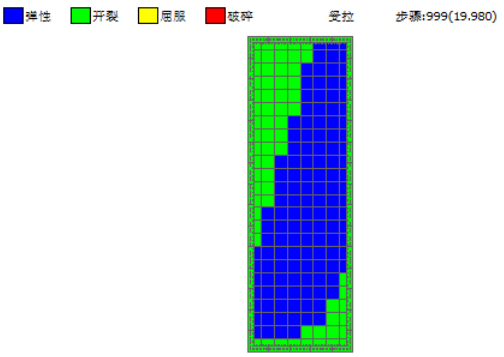

(c) Section at 2/3 height from pier top

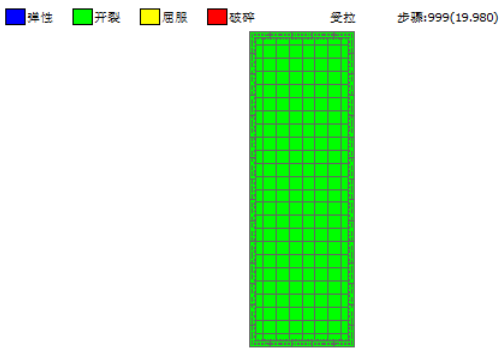

(d) Section at pier base

Fig. 23 - Fiber model analysis results of main pier

(a) Section 1 *(b) Section 2*

Fig. 24 - Fiber model analysis results at the base of the pylon

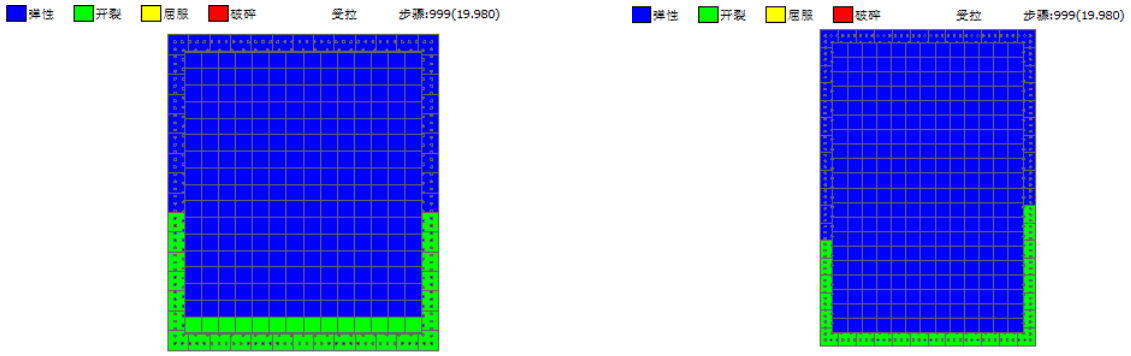

(a) Section 1 *(b) Section 2*

Fig. 25 - Fiber model analysis results of arch foot at 1# pdier

As shown in Figures 23 to 25, the control sections at the consolidation position of the tower, beam, and pier remain in an elastic or locally cracked state under seismic loads, without yielding or fragmentation. This indicates that the consolidation position of the tower, beam, and pier of the bridge has not undergone plastic deformation or damage under seismic action and can resist a certain level of seismic forces, thereby meeting the safety and serviceability requirements of the bridge structure during earthquakes. This result is consistent with the seismic verification results of the substructure.

The conclusions presented in this study are derived from a comprehensive and multi-faceted analytical framework, rather than a single set of seismic response analysis. The research methodology integrated parametric time-history analysis to evaluate the sensitivity of various structural parameters, linear response spectrum analysis for seismic performance verification under E1 seismic actions, and nonlinear elasto-plastic time-history analysis to assess structural behavior and potential damage mechanisms under E2 seismic actions. This integrated approach ensures that the findings and conclusions are robust and well-supported, providing a holistic understanding of the seismic performance of the cable-stayed arch collaborative system bridge.

CONLUSIONS

Based on the theory of structural vibration control and the concept of performance-based seismic design, the concept of time-history response influence factor is proposed. Structural parameter analysis is conducted under three-dimensional seismic loads, and seismic verification of the structure is performed.

(1) The order of sensitivity of the overall seismic performance of the structure to different parameters,

from strongest to weakest, is as follows: inclination angle of the pylon > length of the concrete section of the arch rib > elastic modulus of concrete > layout of wind braces. "K"-shaped wind braces are more beneficial for structural seismic performance compared to parallel wind braces, and the absence of wind braces will have a significant impact on the seismic performance of the structure. Increasing the short length of the concrete section of the arch rib affects the spatial mass distribution of the structure, reducing its overall lateral stability. The use of high-performance concrete can improve the seismic performance of the structure to a certain extent. The originally designed inclination angle of the pylon is closest to the optimal angle.

(2) The wind bracing of the arch ribs develops tensile stress, with maximum tensile stresses of 223.4 MPa (corrected from 176.7 MPa, assuming a typo in the original text), 114.5 MPa, and another value under transverse and longitudinal earthquake actions. Notably, neither the arch ribs nor the wind bracing materials have yielded.

(3) The results of the seismic verification of the bridge structure indicate that both the superstructure and substructure of the bridge can meet the seismic fortification requirements.

(4) The results of the fiber model analysis at the consolidation position of the tower, beam, and pier show that no plastic deformation occurs at this location under seismic action, meeting the seismic requirements of the bridge structure.

REFERENCES

[1] Chai S, Zhang J, Wang X.,2023. Basic Static Behaviours of An Arch-cable Composite Bridge. Structures. Vol. 47, p. 1548-1557. ISSN 2352-0124, https://doi.org/10.1016/j.istruc.2022.11.146

[2] Tian Z, Zhang Z, Ning C., 2024. Multi-objective Optimization of Cable Force of Arch Bridge Constructed by Cable-stayed Cantilever Cast-in-situ Method Based on Improved NSGA-II. Structures. vol. 59, p. 105782. ISSN 2352-0124, https://doi.org/10.1016/j.istruc.2023.105782

[3] Zheng X, Cui Y., 2022. Analysis of Static Performance of Cable-stayed Arch Cooperative Bridge without Back Cable. Archives of Civil Engineering. p. 548-531-548. ISSN 1230-2945

[4] Kang H, Guo T, Zhu W., 2020. Multimodal Interaction Analysis of A Cable-stayed Bridge with Consideration of Spatial Motion of Cables. Nonlinear Dynamics, vol. 99, no. 1, p. 123-147. ISSN 0924-090X, https://doi.org/10.1007/s11071-019-05064-9

[5] Shi Z, Hu H, Li J., 2021. Axis Optimisation of Arch-shaped Pylons for High-speed Railway Cable-Stayed Bridges. Engineering Structures, vol. 227, p. 111424. ISSN 0141-0296, ISSN 0141-0296, https://doi.org/10.1016/j.engstruct.2020.111424

[6] Zheng J., 2024. Recent Construction Technology Innovations and Practices for Large-Span Arch Bridges in China. Engineering, vol. 41. ISSN 2095-8099, https://doi.org/10.1016/j.eng.2024.05.019

[7] Cheng M, Zhang H, Xu H., 2021. Study of Pedestrian Bridge with Flying Swallow–Shaped Arch Rib and Stayed-Cable System. Journal of Highway and Transportation Research and Development (English edition), vol. 15, no. 4, p. 83-89. ISSN 1002-0268, https://doi.org/10.1061/JHTRCQ.0000802

[8] Chen Z, Zhou X, Wang X., 2017. Deployment of A Smart Structural Health Monitoring System for Long-span Arch Bridges: A Review and A Case Study. Sensors, vol. 17, no. 9, p. 2151. ISSN 1424-8220, https://doi.org/10.3390/s17092151

[9] Liu C M, Tserng H P, Teo E H., 2025. Analysis and Sequence for the Cable Design and Construction in Steel Arch Bridges: Lesson Learned from Taipei Chung-cheng Bridge Reconstruction Project. Journal of the Chinese Institute of Engineers, p. 1-15. ISSN 0253-3839, https://doi.org/10.1080/02533839.2024.2420106

[10] Chen C, Yan D, Li Y., 2022. Equivalent Plane Algorithm for Static Analysis of Cable-stayed Bridge with Spatial Cables. Journal of Bridge Engineering, vol. 27, no. 6, p. 04022042. ISSN 1084-0702, https://doi.org/10.1061/(ASCE)BE.1943-5592.000188

[11] Zhang Y, Wang L, Nong Y., 2023. Construction-Monitoring Analysis of a Symmetrical Rigid Frame Tied Steel Box Arch Bridge in Southwest China Based on Segmental Assembly Technique. Symmetry, vol. 15, no. 7, p. 1437. ISSN 2073-8994, https://doi.org/10.3390/sym15071437

[12] Teichgraeber M., 2024. Reliability and Durability Assessment of Bridge Stay Cables. Archives of Civil and Mechanical Engineering, vol. 25, no. 1, p. 29. ISSN 1644-9665, https://doi.org/10.1007/s43452-024-01086-2

[13] Han H J, Guo J P, Zhang J J., 2020. Technical Advances of Temporary Facilities for the Failure Prevention of Large‐Span Cantilever Casting Construction of Mountainous Concrete Box‐Type Arch Bridges. Advances in Civil Engineering, vol. 2020, no. 1, p. 6412613. ISSN 1687-8086, https://doi.org/10.1155/2020/6412613

[14] Pan Q, Yi Z, Zeng Y., 2022. Research on the Free Vibration of the Arch Bridge During Cable Hoisting or Rotation Erection Using An Analytical Modeling. Journal of Vibration Engineering & Technologies, vol. 10, no. 3, p. 1021-1035. ISSN 2523-3920, https://doi.org/10.1007/s42417-021-00426-3

[15] Sun M, Makki Alamdari M, Kalhori H., 2017. Automated Operational Modal Analysis of A Cable-stayed Bridge. Journal of Bridge Engineering, vol. 22, no. 12, p. 05017012. ISSN 1084-0702, https://doi.org/10.1061/(ASCE)BE.1943-5592.0001141

[16] Su H, Guo C, Han T., 2023. Research on Safety State Evaluation of Cable-Stayed Bridge Structures across the Sea. Journal of Marine Science and Engineering, vol. 11, no. 11 p. 2034. ISSN 2077-1312, https://doi.org/10.3390/jmse11112034

[17] Yi Z, Yuan M, Tu G., 2019. Modeling of the Multi-cable Supported Arch and A Novel Technique to Investigate the Natural Vibratory Characteristics. Applied Mathematical Modelling, vol. 75, p. 640-662. ISSN 0307-904X, https://doi.org/10.1016/j.apm.2019.05.055

[18] Kang H, Su X, Pi Z., 2022. Planar Nonlinear Dynamic Analysis of Cable-stayed Bridge Considering Support Stiffness. Nonlinear Dynamics, vol. 107, no. 2, p. 1545-1568. ISSN 2077-1312, https://doi.org/10.1007/s11071-021-06381-8

[19] Zhang W, Chen J, Chang J., 2023. Analytical Assessment of the Full-bridge Response to the Vertical Live Load: An Algorithm for Hybrid Cable-stayed Suspension Bridges. Advances in Structural Engineering, vol. 26, no. 16, p. 3021-3040. ISSN 1369-4332

[20] Tian Z, Cai Y, Peng W., 2024. Multi-loop Nesting Algorithm and Response Analysis of Cable Forces of Long Span Cantilever Cast Arch Bridges during Construction. KSCE Journal of Civil Engineering, vol. 28, no. 2, p. 699-714. ISSN 1226-7988, https://doi.org/10.1007/s12205-023-1970-3